Heliyon 9 (2023) e12942

Contents lists available at ScienceDirect

Heliyon

journal homepage: www.cell.com/heliyon

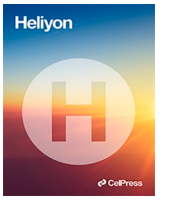

Research article

Simultaneous effects of MWCNT and SiO2 on the rheological behavior of cooling oil and sensitivity analysis

Mousa Rejvani [a,*], Alireza Heidari [b], Seyfolah Seadodin [a]

[a] Department of Mechanical Engineering, Semnan University, Semnan, Iran
[b] Department of Mechanical Engineering, Damghan University, Damghan, Iran

ARTICLE INFO

Keywords:
Characterization
Hybrid nano-lubricants
Viscosity
Sensitivity
RSM Modeling
Nanofluid

ABSTRACT

Many scholars are attracted to nano-lubricants due to their unique properties. In the present study, the rheological behavior of a new generation of lubricants has been investigated. SiO_2 nanoparticles with an average diameter of 20–30 nm along with MWCNT with an internal diameter of 3–5 nm and the external diameter of 5–15 nm has been dispersed in 10W40 engine oil as base-lubricant and MWCNTs-SiO2 (20%–80%)/10W40 hybrid nano-lubricant has been produced. Nano-lubricant behavior agrees with the Herschel-Bulkley model and is of Bingham pseudo-plastic type below 55°*C*. Also, in the temperature of 55°*C*, nano-lubricant behavior has changed to Bingham dilatant. The viscosity is increased by 32% in the proposed nano-lubricant compared to base lubricant (Dynamics Viscosity Enhancement). Finally, a new correlation with a precision index of R-squared >0.9800, Adj. R-squared >0.9800, and the maximum margin of deviation of 2.72% has been presented, increasing the applicability of this nano-lubricant. Eventually, the sensitivity analysis of nano-lubricant has been conducted, studying the comparative effect of volume fraction and temperature on viscosity.

1. Introduction

Nanofluid refers to a stationary fluid in which particles in nanoscale are suspended and dispersed [1]. Today, nanofluids are used in thermal issues in various cases, which is due to the presence of intra-fluid solid nanoparticles which greatly affect thermal performance in heat transfer applications [2-8]. But the important point of nanofluids application in thermal equipment is their appropriate production to overcome some problems namely corrosion, agglomeration, erosion, and instability [9-14].

Recently scholars, considering unique thermal properties of nanofluids, have focused on nanofluids. Thus, determining the thermophysical properties and rheological behavior of nanofluid to make them applicable in the industry becomes very important. The lubricating power of nanofluids in addition to their unique thermal properties [15-20] are the reason for using them in different industries such as thermal transformers, military, and electronic [21-24]. One substantial parameter affecting nanofluids thermo-physical properties is their viscosity. Viscosity means friction resistance against shear stress. The resistance lies between the adjacent layers of a fluid. The rheological behavior of nanofluids, which is, in fact, the behavior of fluid transformation in mechanical stress conditions, has a determining role in their application since whether a fluid is Newtonian or not greatly affects its thermo-physical properties [25-27]. The more volume fraction of nanoparticles in base fluid, the more thermal conductivity and viscosity. Also, increase in nanofluid temperature greatly promotes thermal conductivity [28-32]. On the other hand, increasing

* Corresponding author.
E-mail address: m.rejvani@semnan.ac.ir (M. Rejvani).

https://doi.org/10.1016/j.heliyon.2023.e12942
Received 9 March 2022; Received in revised form 26 November 2022; Accepted 9 January 2023
Available online 12 January 2023

nanoparticle density and decreasing nanofluid temperature, boost the nanofluid viscosity [14,25,33–40]. Therefore, nanofluids rheological behavior can be considered as a significant factor affecting heat transfer, efficiency, and also costs.

In Table 1, a summary of studies on nanofluids non-Newtonian behavior has been presented.

In Table 2, a summary of studies on nanofluids thermo-physical properties has been presented.

Today, researchers extensively conduct studies on carbon nanoparticles such as graphite SWCNT [41-44], CNT [27,45,46], MWCNT [47,48] and graphene [49-53]. The reason is significant thermal and rheological properties of this type of nanoparticles. However, due to the high costs of carbon nanoparticles production, their usage is not recommended. In the recent years, one of the most challenging issues for researchers has been the commercialization of nanofluids in different applications. The studies of researchers in the last decade have moved toward using a combination of oxide and carbon nanoparticles since this type of nanofluids which is known as hybrid nanofluids, as well as keeping thermal performance and high lubricating properties, has lower production costs compared to carbon nanofluids. The review of the literature reveals that examining thermo-physical properties and rheological behavior of this type of nanofluids has not been seriously considered. In the present study, the rheological behavior of MWCNTs-SiO_2 (20%–80%)/10W40 hybrid nano-lubricant with a change of temperature and nanoparticles volume fraction has been investigated, and acceptable results have been obtained. In this research, for the first time, hybrid nano-lubricant MWCNTs-SiO_2 (20%–80%)/10W40 with non-Newtonian (Bingham) behavior from pseudo-plastic type has been introduced. Studying the interaction between the particles in nanofluids leads to a nonlinear relationship between viscosity, volume fraction and temperature [54-57]. Eventually, due to the non-Newtonian behavior of nano-lubricant, a new correlation as modeling and sensitivity analysis has been presented, increasing engineering applicability.

2. Experiments

Engine oil is used to reduce friction and improve the heat transfer in moving parts. The nano-lubricant, with engine oil as the base fluid, are used to increase the viscosity at high temperatures along with improving thermal features. Viscosity and lubrication are the primary functions of the nanofluids' application. On the other hand, nanofluid could improve thermal efficiency at high temperatures.

Spherical nanoparticles, e.g., SiO2, play a vital role in promoting lubrication, while cylindrical nanoparticles, such as MWCNT, far less can improve the lubrication in rolling mode. Cylindrical nanoparticles are mainly used to increase the thermal conductivity coefficient in addition to the benefits of lubrication. Furthermore, compared to SiO2 and the performance, MWCNT has a high production cost.

From a cost point of view, the production of nano-lubricants with 100% of carbon nanotubes individually has no economic feasibility at all that has not been done in any research. Since, it does not have the desired lubrication, which is the main function of nano-lubricants. On the other hand, the production of nano-lubricants by 100% of SiO2 nanoparticles will not have the thermal efficiency of hybrid ones. Consequently, it is clear that the use of hybrid nano-lubricants will be more efficient and feasible.

Accordingly, SiO2 was used together with MWCNT in the ratio of 80–20% in this research regarding the importance of lubrication efficiency, thermal conductivity and the cost of production. Hybrid nano-lubricant was prepared by dispersing 80% SiO_2 oxide nanoparticles and 20% multiwall carbon nanotube (MWCNT) in 10w40 lubricating oil. The question may arise as to what is the main reason behind the use of 80–20% of SiO2-MWCNT in this study.

As discussed, carbon nanotubes cannot take the higher share, so it is used as an additive to the lubricants. Therefore, 50-50% and 60-40% are not feasible considerations and the experiments can be done on 90–10, 80–20, and 70–30 percentages. The large amount of the experimental data related to each of these feasible compositions could be analyzed through individual research, then the comparison between the results and choosing the most optimal combination would be a good research question in a further study. Accordingly, we could assess one these feasible compositions (90–10, 80–20, 70–30) through this study. Among these, we choose 80–20 as the average percentage, which can be a reasonable choice.

Table 1
Summary of studies on the non-Newtonian rheological behavior of nanofluids.

Author(s)	Base fluid	Dispersed particle	Conc. (vol %)	Temp.	Diameter (nm)	Rheological behavior
Jamal-Abad et al. [66]	*Oil*	*CuO* *Al_2O_3* *TiO_2*	*1 & 2*	*15.6*	*40* *15* *20*	*Shear thinning*
Wang et al. [67]	*[Bmim][PF6]*	*MWCNT*	*0-0.1 wt%*	*Ambient temperature*	*Diameter: 20*–40 nm *Length: 5*–15 μm	*Low concentration: shear thinning* *High concentration: Newtonian*
Abareshi et al. [68]	*glycerol*	*Fe_2O_3*	*0.25–0.8*	*25*	*26*	*Shear thinning*
Chen et al. [69]	*EG*	*TNT*	*0–8*	*20–60*	*10*	*Shear thinning*
Afrand et al. [70]	*EG*	*Fe_3O_4–Ag*	*0.0375–1.2*	*25–50*		*Shear thinning*
Kole and Dey [71]	*EG-water*	*Al_2O_3*	*0.1–1.5*	*10–50*	*50*	*Bingham plastic*
Tseng et al. [59]	*water*	*TiO_2*	*5–12*	*25*	*7–20*	*Shear thinning*
Eshgarf et al. [72]	*EG-water*	*COOH functionalized MWCNTs -SiO2*	*0.0625–2*	*Ambient temperature*	*20*–30 nm *Inner diameter 5*–15 nm	*Shear thinning*

Table 2
Summary of studies on the thermos-physical properties of nanofluids.

Ref.	Base fluid	Nanoparticle	Temp. (°C)	Conc. (%)
Sun et al. [73]	water	SiO2	21	1.96–12.85
Ettefaghi et al. [60]	SAE20W50	MWCNT	40–100	0.1,0.2,0.5 wt
Fakoor Pakdaman et al. [17]	Heat transfer oil	MWCNT	40–100	0.4 wt
Pakdaman et al. [17]	Heat transfer oil	MWCNT	40–70	0.1,0.2,0.4 wt
Glory et al. [74]	water	MWCNT	15–75	0.24
Hemmat esfe et al. [75]	Water	MWCNT	25–55	0.05–1
Pang et al. [76]	Methanol	SiO2	20	0.01–1

On the one hand, the 70-30% SiO2-MWCNT nano lubricant, due to the presence of more carbon nanotubes, reduces the stability of the suspension and increases the issues related to sedimentation and agglomeration. On the other hand, the 90-10% combination decreases the thermal benefits of MWCNTs. Over all, the 80-20% can be considered as a reasonable assumption for this study and the other two feasible combinations (70-30% and 90-10%) and their comparison could be a proper research question for further individual studies.

In order to calculate volume fractions, equation (1) has been used. The properties of nanoparticles and lubricant oil 10w40 have been presented in Tables 3–5.

$$\varphi = \frac{\frac{w}{\rho}\Big|_{MWCNT} + \frac{w}{\rho}\Big|_{SiO_2}}{\frac{w}{\rho}\Big|_{MWCNT} + \frac{w}{\rho}\Big|_{SiO_2} + \frac{w}{\rho}\Big|_{10W40}} \tag{1}$$

Stabilization process is necessary to achieve the optimal performance of the nano-lubricant in different laboratory conditions. For this purpose, initial dispersion and homogenization were performed using a magnetic stirrer for 3 h. The agglomerated nanoparticles were then removed by an ultrasonic homogenizer. The required equipment for the stabilization process of nano lubricant is illustrated schematically in Fig. 1a.

Estimating the relative stability of nanofluids benefits from different methods and tools, e.g. densitometry test (sediment imaging), spectrophotometer, sediment balance method, TEM, and SEM. This study enjoys densitometer to evaluate the deposition of nanoparticles in the base fluid and the stability of the nano lubricants. Hence, the lower and the upper parts of the samples were examined in different volumes, three times a week. It comes to the conclusion that the percentage of sediment in all volume fractions of the samples was negligible (0.01%). The reason for the and acceptable stability quality of the samples could be the Initial homogenization using a magnetic stirrer as well as decomposition of residual cluster using an ultrasonic homogenizer.

In Fig. 1b, samples of XRD and transmission electron microscopy (TEM) of SiO_2 oxide nanoparticles and MWCNTs nanoparticles are exhibited. The average diameter of SiO_2 as oxide nanoparticles has been 20–30 nm and internal and external diameters of MWCNTs have been obtained 3–5 and 5–15 nm, respectively.

First, SiO_2 and MWCNTs nanoparticles are weighed, considering the percentage of their mixture (80% and 20%, respectively) and maximum volume fraction (1%) by a digital scale with the precision of 0.01 gr. After combining nanoparticles with each other, the sample is mixed with 10w40 lubricant oil. To have a better mixture of nanoparticles and oil solvent, MWCNTs-SiO_2 (20%–80%)/10W40 nano-lubricant has been prepared in a two-step method. First, the mixture was processed with a magnetic processor for 75 min. In order to break down the clustering and agglomerations between nanoparticles inside the solution, a 800 W ultrasonic processor in the frequency of 20 kHz was used for 265 min. In Fig. 2, densitometer, SiO_2 and MWCNT nanoparticles, Scanning Electron Microscope (SEM) of them, and stable samples prepared in different volume fractions have been shown.

2.1. Viscosity measurement

The viscosity of the pure oil and hybrid nano-lubricant in volume fractions of 0.05%–1% was measured. In this experiment, the dynamic viscosity of samples was measured with changing the shear rate from $666.665s^{-1}$ to $13333.3s^{-1}$ in temperatures of 5 to$55^{\circ}C$. In order to perform the experiment, Brookfield viscometer (Cap 2000+), made in the U.S., has been used, which has the precision of ± 1.0% and repeatability of ±0.5%.

Table 3
Physicochemical property of silicon dioxide (SiO2) nano-powder.

Property	Value
Purity	99.5%
APS	20–30 nm
Color	White
SSA	180–600 m^2/g
Bulk density	<0.10 g/cm^3
True density	3.4 g/cm^3

Table 4
Physicochemical characteristics of MWCNTs.

Parameter	Value
Color	Black
Purity	>95 wt% (carbon nanotubes) (from TGA & TEM) >97 wt% (carbon content)
Length	~50 μm (TEM)
Tap density	0.27 g/cm^3
True density	~2.1 g/cm^3
Outside diameter	5–15 nm (from HRTEM, Raman)
Inside diameter	3–5 nm
SSA	>233 m^2/g (BET)
Thermal conductivity	1500 W/m K
Electrical conductivity	>100 s/cm

Table 5
Engine oil (10W40) characteristics.

Parameter	Value
Density at 60 °F (15.6 °C)	827 kg/m^3
Sulfated ash	0.86%
Neutralization No. (TBN-E)	7.1
Viscosity index	149
CCS viscosity at −13 °F (−25 °C)	6270 cP
Kinematic viscosity at 100 °F (38 °C)	108.5 cSt
Kinematic viscosity at 210 °F (99 °C)	15.4 cSt
Flashpoint	220 °C
Pour Point	−33 °C

3. Result and discussion

3.1. Rheological behavior investigation

One of the factors affecting the thermal conductivity of fluids, convection heat transfers of fluids, and also pressure drop and pumping power is the rheological behavior of that fluid. Lubrication power of fluids is a function of their rheological behavior. Therefore, recognizing the behavior of fluids is of great importance.

In order to recognize the rheological behavior type of each fluid, the amount of apparent viscosity and shear stress of that fluid are investigated with changes in shear rate. Apparent viscosity and shear stress of nano-lubricant MWCNTs-SiO2 (20%–80%)/10W40 and pure oil 10W40 are illustrated as in Fig. 3. According to non-linear changes in apparent viscosity and shear stress in terms of shear rate, it can be mentioned with certainty that this nano-lubricant has shown non-Newtonian behavior. However, due to lack of sufficient precision in the figure, non-Newtonian type of nano-lubricant is not recognizable.

As a result, in order to have a precise recognition of non-Newtonian behavior of nano-lubricant, Herschel-Bulkley model [58] and Ostwald de Walde function are used as equation (2).

$$\begin{aligned} &\tau_{OW} = m\dot{\gamma}^n \\ &m = Consistency\ index \\ &n = Power\ law\ index \end{aligned} \tag{2}$$

Equation (2) can be used for the fluids that lack yield stress, and the change of shear stress in terms of shear rate is drawn from the origin of coordinate. If $n = 1$, the fluid is Newtonian since its shear stress variations in terms of shear rate are linear. If $n > 1$ or $n < 1$, it shows the non-Newtonian behavior of pseudo-plastic (shear thinning) and dilatant (shear thickening), respectively.

If the fluid has a non-Newtonian behavior and yield stress, when shear stress variations begin after yield stress, equation (3) is used.

$$\begin{aligned} &\tau_{HB} = \tau_y + K\dot{\gamma}^t \\ &\tau_y = Yield\ stress \\ &t, K = Structure - dependent\ parameters \\ &\dot{\gamma} = Shear\ rate \end{aligned} \tag{3}$$

This type of behavior is referred to as Bingham. If $t < 1$, it is called Bingham non-Newtonian fluid with pseudo-plastic type, and if $t > 1$, it is called Bingham non-Newtonian fluid with dilatant type. If $t = 1$, shear stress changes in terms of the shear rate will be linear and with initial yield stress. In order to exactly determine the type of behavior of MWCNTs-SiO_2 (20%–80%)/10w40 nano-lubricant, these two models must be fitted on the data of shear rate graphs in terms of shear stress (Fig. 3). By investigating the amount of precision and agreement of each of the two models with the data, the exact behavior of nano-lubricant is determined. In order to examine the agreement of the two models with the data, their R-squared values have been presented in Tables A and B (appendix).

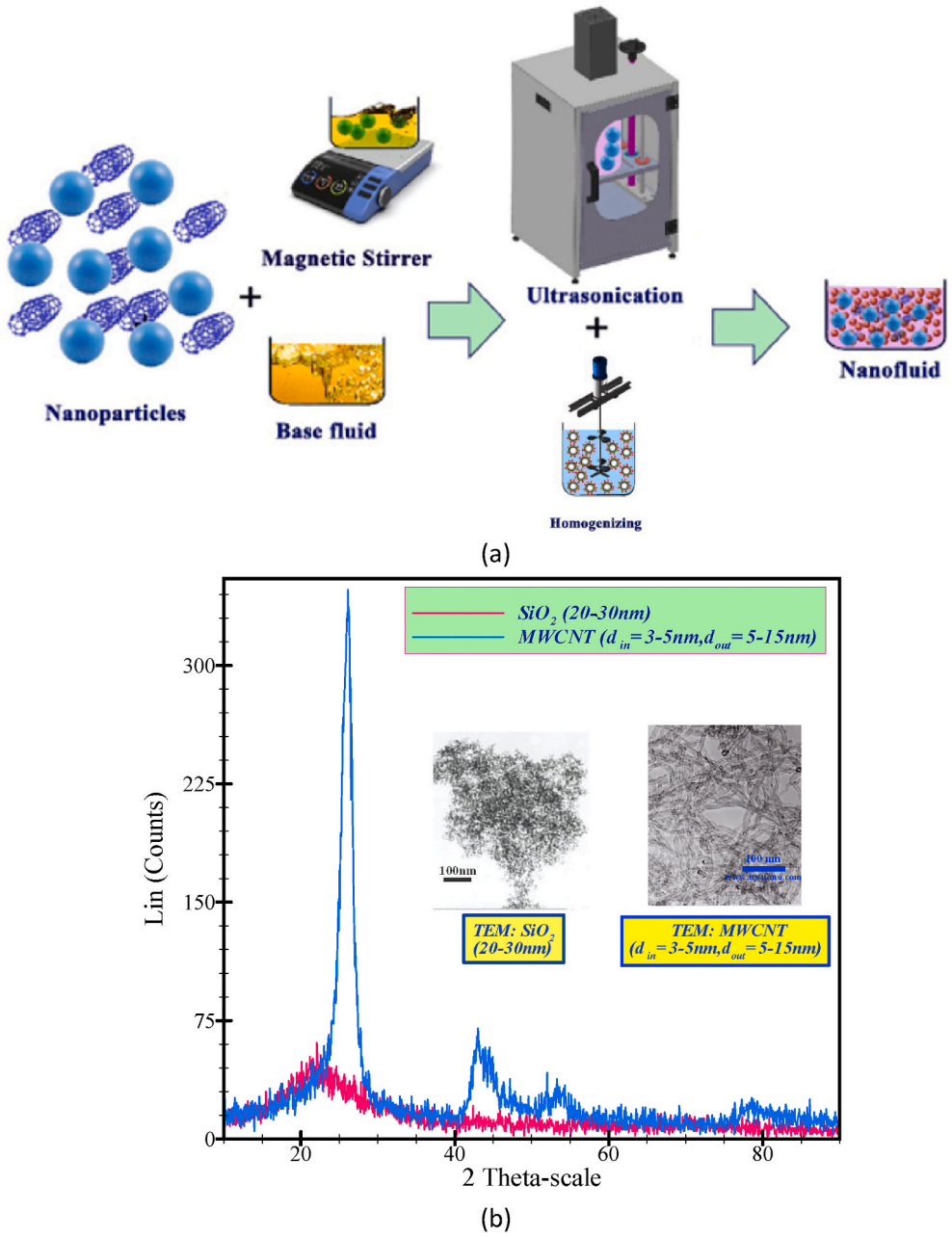

Fig. 1. a) The required equipment for the stabilization process of nano lubricant b) XRD pattern and TEM analysis for MWCNTs and SiO_2 nanoparticles.

Also, in T. C, the difference in R-squared values obtained from these two models has been shown. According to Table C, the number of positive numbers in this table are more than that of negative ones. This means that, in the most part of the data, fitting process of Herschel-Bulkley model has a better agreement compared to Waele Ostwald de model. So, the behavior of MWCNTs-SiO_2 (20%–80%)/10W40 nano-lubricant can be considered as Bingham.

In Tables 6–8, the coefficients related to Bingham model (structure-dependent parameters and yield stress values) have been presented. According to Table 8, the exact behavior of MWCNTs-SiO2 (20%–80%)/10W40 nano-lubricant is of pseudo-plastic type. In order to show the percentage of behavior deviation of nano-lubricant from Bingham linear behavior to pseudo-plastic non-linear behavior, Table 9 has been presented.

As observed in Fig. 4, change in yield stress with increasing volume fraction and the temperature of 5–45°*C* is small. In this part, the coefficients are almost zero. With increasing temperature up to 55°*C*, yield stress becomes positive. Also, in 55°*C*, increasing volume fraction has shown a great change in yield stress to over 100 Pa. This great change occurs due to a change in the level of energy of

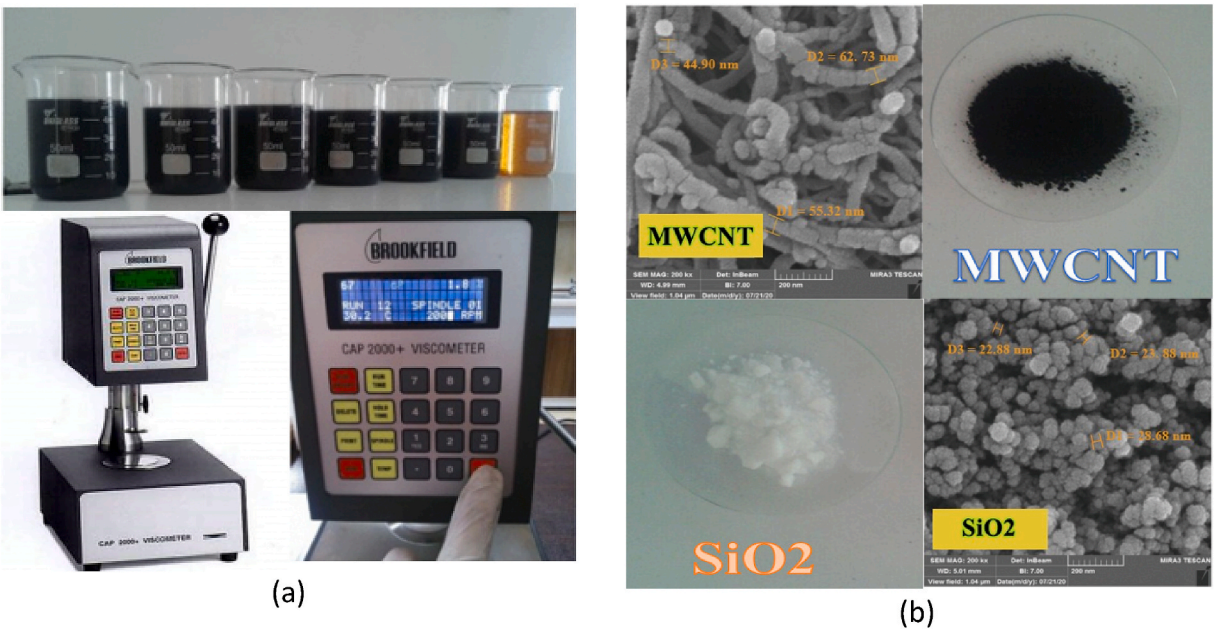

Fig. 2. a) Nano-lubricant samples and densitometer b) SiO_2 nanoparticles and MWCNTs SEM.

nanoparticles inside the nano-lubricant. In the study of Tseng and Lin [59], similar results have been obtained for TiO2/water nanofluid.

For the shear stress lower than yield stress, nano-lubricant can be resistant against it. This behavior is due to the three-dimensional structure of the material. In fact, by dispersing nanoparticles in oil, some contact appears inside nano-lubricant. Owing to the contacts, a false body of nanoparticles, which is a solid and weak structure, is formed inside nano-lubricant. For the nano-lubricant to move, this structure has to be broken down. In fact, yield stress is for breaking down this structure. As shown in Fig. 4, yield stress is not zero in any of the experiment samples. This is the reason for non-Newtonian (Bingham) behavior of nano-lubricant.

As observed in Fig. 5, changes in "K" have been shown in different temperatures and volume fractions. "K", in temperatures of 5–55°C has decreased while increasing temperature. Also, with increasing volume fraction, almost no change is seen in "K", while in different temperature, decreasing volume fraction to 0.1% shows an increase in "K". In this volume fraction, the second term of Herschel-Bulkley model, ($K\dot{\gamma}^t$), has the greatest effect on nano-lubricant stress. In 55°C, due to small values for K, the effect of the second term of Herschel-Bulkley model, ($K\dot{\gamma}^t$), is so small. In other words, nano-lubricant yield stress is equal to shear stress ($\tau_{HB} = \tau_y$). In this condition, yield stress has significant impact on determining the rheological (non-Newtonian) behavior of hybrid nano-lubricant.

Fig. 6 shows variations of "t" index in terms of volume fraction and temperature. As seen in the figure, "t" index is less than one except in 55°C. These values show Bingham non-Newtonian behavior of pseudo-plastic type. In this temperature, "t" values have become greater than 1 and hybrid nano-lubricant behavior has suddenly turned to dilatant behavior. In this figure, the effect of temperature and volume fraction on the rheological (non-Newtonian) behavior of nano-lubricant is properly demonstrated.

3.2. *The effects of concentration and temperature on dynamic viscosity*

In Fig. 7, viscosity variations in terms of different temperatures and volume fractions have been shown in a certain shear rate. van der Waals intermolecular forces caused SiO_2 oxide nanoparticles and MWCNTs carbon nanotubes to lie next to each other and form nanoclusters. The presence of these nanoclusters in base lubricant increases friction between the layers of lubricant. Therefore, lubricant moves with more difficulty. So we can expect that with increasing volume fraction, viscosity increases.

Also, viscosity decreases with increasing temperature because increasing temperature increases the speed and movement of particles and as a result decreases adhesion force between nanoparticles and molecules. So the friction between the layers of nano-lubricant is reduced and this will decrease the viscosity.

In addition, as observed in Fig. 7, nano-lubricant viscosity in each temperature and volume fraction is greater than base oil viscosity. For instance, nano-lubricant viscosity in the highest volume fraction (1%) and lowest temperature (5°C) is over 1.3 times as big as that of pure oil. And in the lowest volume fraction (0.05%) and highest temperature (55°C), it is equal to pure oil.

To investigate the variations of the viscosity of MWCNT-SiO_2 (20%–80%)/10W40 nano oil due to volume fraction and temperature, equations (4) and (5) can be used.

$$\Delta\mu_{\varphi} = \mu_{\varphi_{\max}} - \mu_{\varphi_{\min}} \tag{4}$$

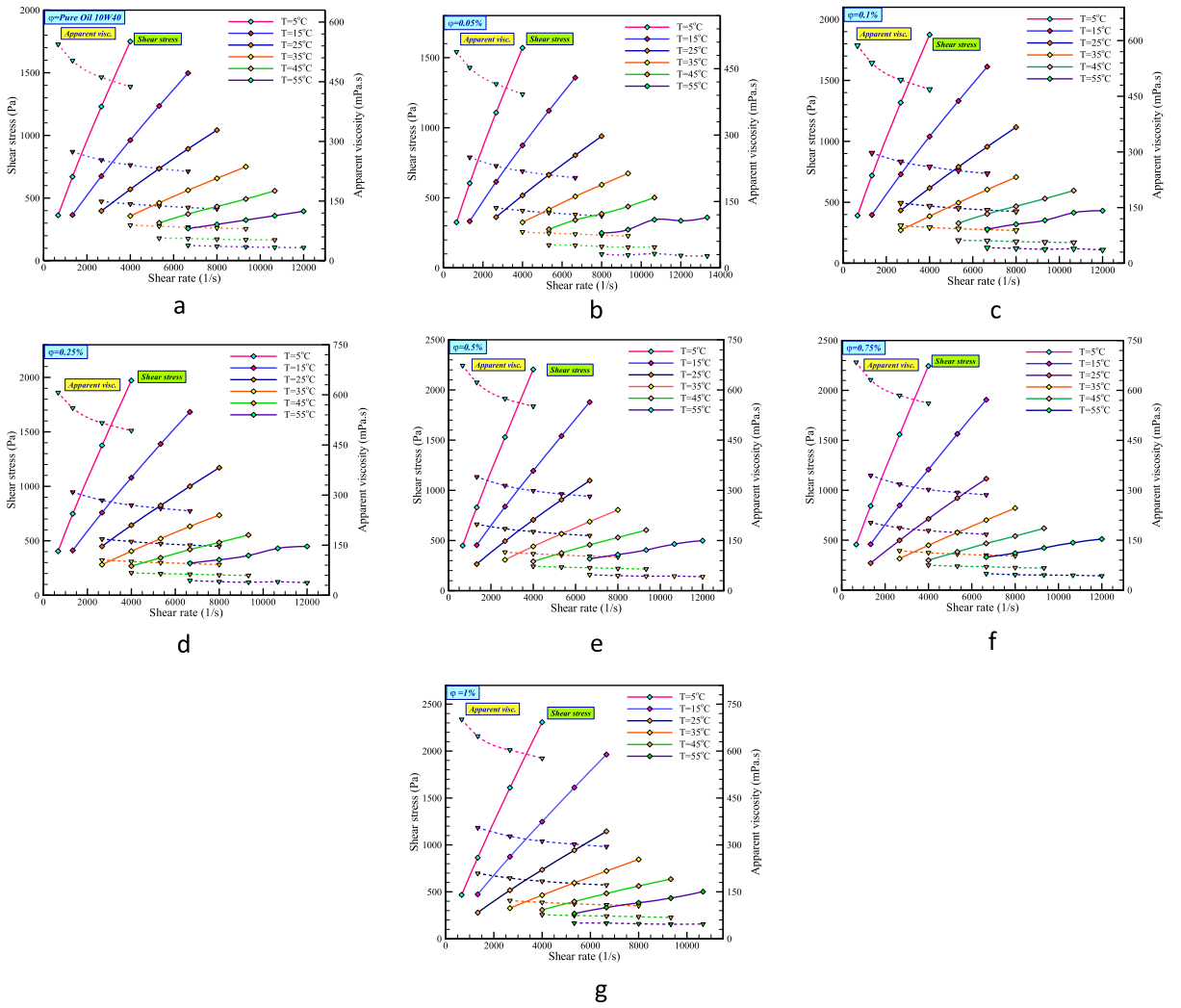

Fig. 3. Shear Stress and Apparent viscosity at constant shear rate in terms of temperature and solid volume fractions: a) φ = 0 b) φ = 0.05 c) φ = 0.1 d) φ = 0.25 e) φ = 0.5 f) φ = 0.75 g) φ = 1.

Table 6
Yield-stress (mPa.s) factor Herschel-Bulkley model for hybrid nano-lubricant.

Yield stress	Solid volume fraction (%)						
T (°C)	1	0.75	0.5	0.25	0.1	0.05	0
5	0.7981	15.31	16.7	4.064	0<	0<	0<
15	5.393	11.61	6.189	0<	0<	0<	0<
25	0<	0<	0<	0<	0<	0<	0<
35	0<	0<	0<	0<	0<	0<	0<
45	0<	0<	0<	0<	0<	0<	0<
55	32.54	64.63	90.12	99.85	0<	0<	47.74

Equation (4) evaluates the difference between the viscosity of the highest volume fraction and the viscosity of the lowest volume fraction in each temperature.

$$\Delta\mu_T = \mu_{T_{\min}} - \mu_{T_{\max}} \tag{5}$$

Also, equation (5) calculates the difference between the viscosity of the highest temperature and viscosity of the lowest temperature in each volume fraction.

In Fig. 8, the effect of temperature and volume fraction on dynamic viscosity of nano-lubricant in a certain shear rate (as an example $3999.99s^{-1}$) has been shown. The difference in dynamic viscosity has increased with increasing volume fraction. Also, increasing

Table 7
K INDEX (mPa.s^t) factor Herschel-Bulkley model for hybrid nano-lubricant.

K INDEX	Solid volume fraction (%)						
T (°C)	1	0.75	0.5	0.25	0.1	0.05	0
5	1.402	1.242	1.217	1.252	*1.35*	*1.24*	1.236
15	0.7811	0.7119	0.7487	0.7778	0.7788	0.713	0.9634
25	0.5315	0.4842	0.4933	0.4736	0.5004	0.434	0.4041
35	0.3418	0.3246	0.3146	0.2952	0.2699	0.02856	0.2627
45	0.2651	0.25	0.2464	0.2302	*0.2328*	*0.0355*	0.171
55	0.0585	0.0872	0.02673	0.01644	0.302	0.4485	0.1047

Table 8
t INDEX factor Herschel-Bulkley model for hybrid nano-lubricant.

T INDEX	Solid volume fraction (%)						
T (°C)	1	0.75	0.5	0.25	0.1	0.05	0
5	0.893	0.9033	0.9036	0.8873	0.8724	0.8724	0.8749
15	0.8889	0.8957	0.8887	0.8723	0.8673	0.8681	0.8721
25	0.8717	0.8796	0.8755	0.8694	0.8579	0.8648	0.8743
35	0.8695	0.8719	0.873	0.8706	0.8762	1.107	0.8707
45	0.8515	0.8549	0.8539	0.8519	0.8461	1.024	0.872
55	0.9686	0.9103	1.027	1.063	0.7747	0.716	0.8626

Table 9
Percentage of non-Newtonian (pseudo-plastic) rheological behavior.

Pseudo-plastic (%)	Solid volume fraction (%)						
T (°C)	1	0.75	0.5	0.25	0.1	0.05	0
5	10.7	9.67	9.64	11.27	12.76	12.76	12.51
15	11.11	10.43	11.13	12.77	13.27	13.19	12.79
25	12.83	12.04	12.45	13.06	14.21	13.52	12.57
35	13.05	12.81	12.7	12.94	12.38	10.7-	12.93
45	14.85	14.51	14.61	14.81	15.39	−2.4	12.8
55	3.14	8.97	2.7-	6.3-	22.53	28.4	13.74

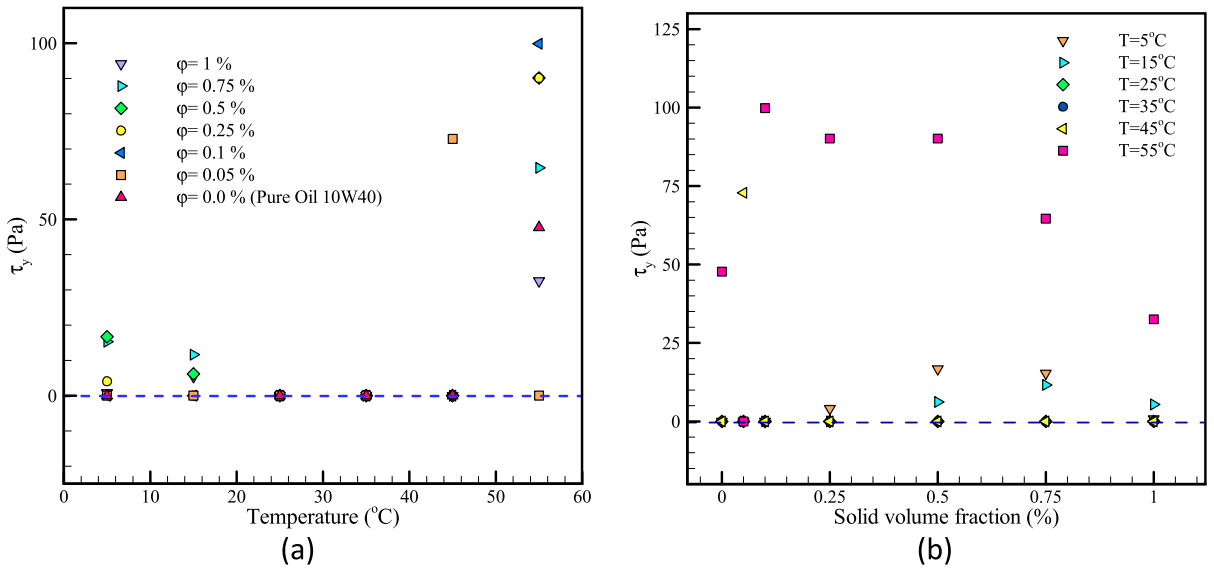

Fig. 4. Yield stress coefficient in terms of a) temperature and b) solid volume fraction.

temperature has decreased the difference in dynamic viscosity. In fact, with increasing temperature, the sensitivity of viscosity to volume fraction decreases. In other words, in high temperatures, adding nanoparticle to lubricant does not show a great change in viscosity, while the effect of volume fraction in lower temperatures cannot be ignored.

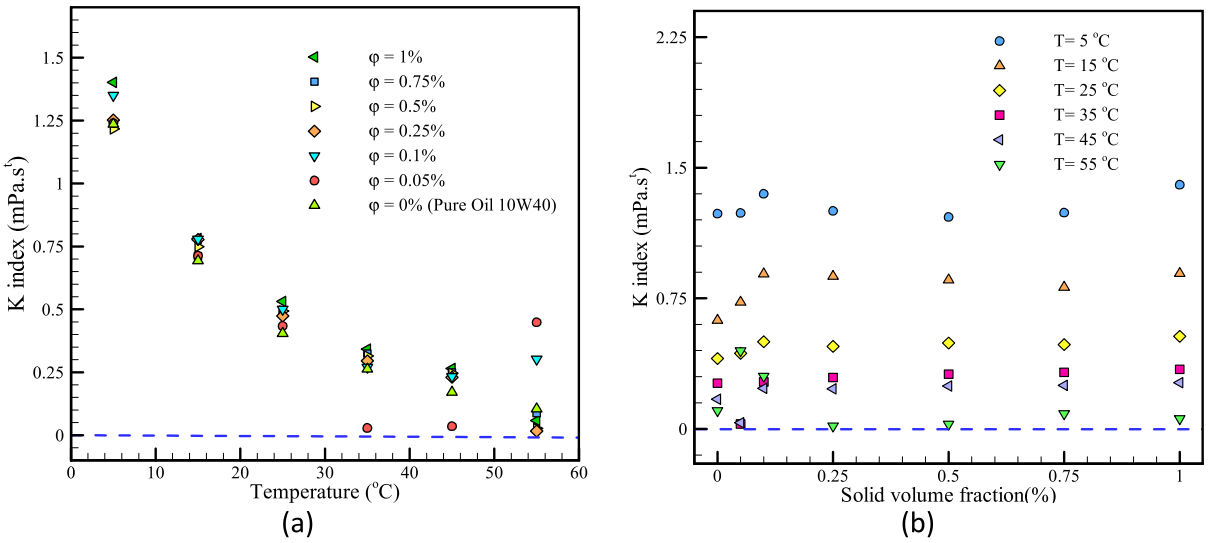

Fig. 5. Variation of K index in terms of a) temperature and b) solid volume fraction.

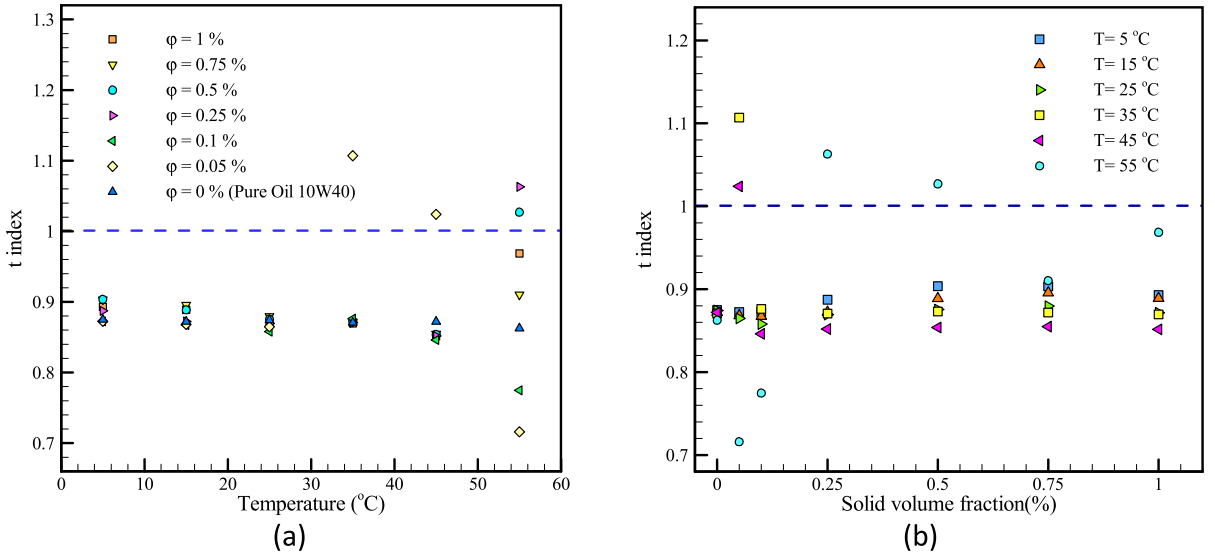

Fig. 6. Variation of t index in terms of a) temperature and b) solid volume fraction.

Fig. 9 shows variations of Dynamic Viscosity Enhancement (DVE) in temperatures and volume fractions in the experiment. Adding nanoparticle to the oil has increased the DVE value in nano-lubricant. This is due to the increase in the friction between the layers of nano-lubricant, which is caused by the extensive presence of nanoparticles in the lubricant. In fact, friction increase has led to an increase in the viscosity of nano-lubricant and in turn DVE has increased. As observed in the figure, the highest DVE has difference of about 32% compared to the base lubricant. This great increase can be used in some parts of industry which require a lubricant with high viscosity [60].

3.3. Proposed correlation

In order to predict and estimate nano-lubricant relative viscosity exactly (Fig. 10), a new experimental correlation has been proposed, due to the weakness of data prediction of the existing theoretical models. This correlation model, equation (6), predicts the relative viscosity in terms of temperature and volume fraction of nano-lubricant.

$$\mu_{nf}/\mu_{bf} = b_0 + b_1\varphi + b_2\varphi^2 + b_3\varphi^3 \tag{6}$$

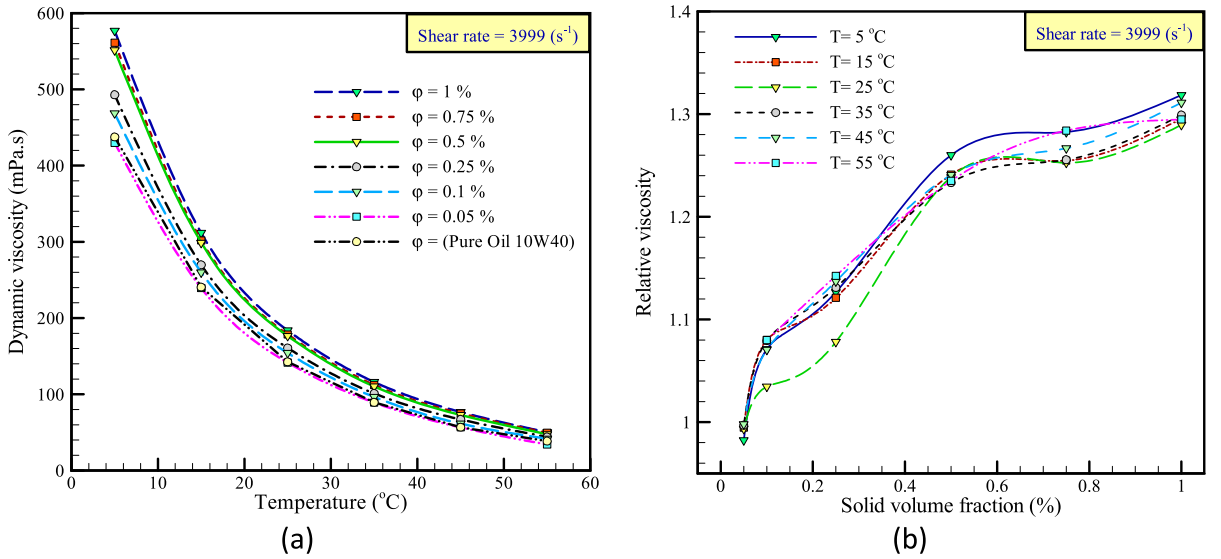

Fig. 7. Dynamic and relative viscosity at constant shear rate versus a) temperature and b) solid volume fraction.

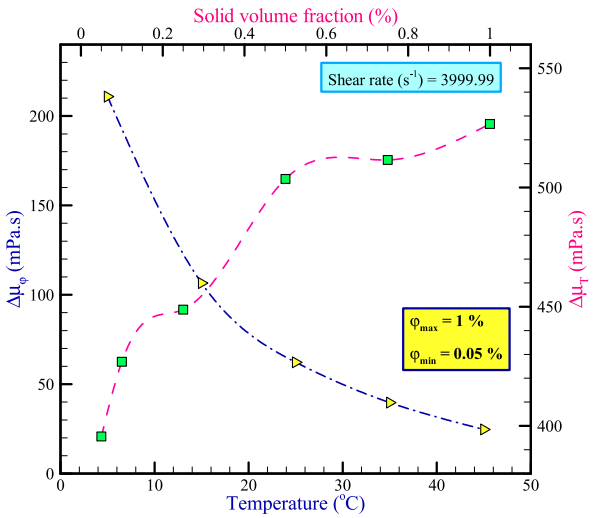

Fig. 8. The dynamic viscosity differences in terms of temperature and solid volume fraction at constant shear rate.

In this correlation, μ_{nf} is nanofluid viscosity, μ_{bf} is base fluid viscosity, $\frac{\mu_{nf}}{\mu_{bf}}$ is relative viscosity, φ is nanoparticle concentration (%). This correlation has been obtained using ANOVA analyzes. In Table 10, the value of precision of each of the parameters in the correlation and also the precision of correlation in terms of different indexes of R-squared and Adj. R-squared have been shown. Table 7 shows the constant variables of the correlation.

According to Fig. 10, the theoretical models of Brinkman [61], Chen et al. [62], Wang et al. [63], and Einstein [64] have been used to predict the relative viscosity of hybrid nano-lubricant. Also, in this figure, the experimental data in 35 °C have been compared with the present theoretical models and the proposed experimental model in this study. Seemingly, none of the present theoretical models can predict experimental data, while the proposed correlation agrees with the experimental data with a high precision.

Relationship 6 is acceptable for temperatures of 5–55 °C and volume fractions of 0.05%–1%. Equation (7) has been used to calculate Margin of Deviation (MOD) of the predicted data.

$$MOD(\%) = \frac{\mu_{rel}|_{Exp.} - \mu_{rel}|_{pred.}}{\mu_{rel}|_{Exp.}} \times 100 \tag{7}$$

In Fig. 11a, MOD values in terms of temperature and volume fraction of nanoparticles have been shown. According to this figure, the maximum of MOD is 2.72% in 55°C and volume fraction of 0.1%. According to this figure, the proposed correlation has a high

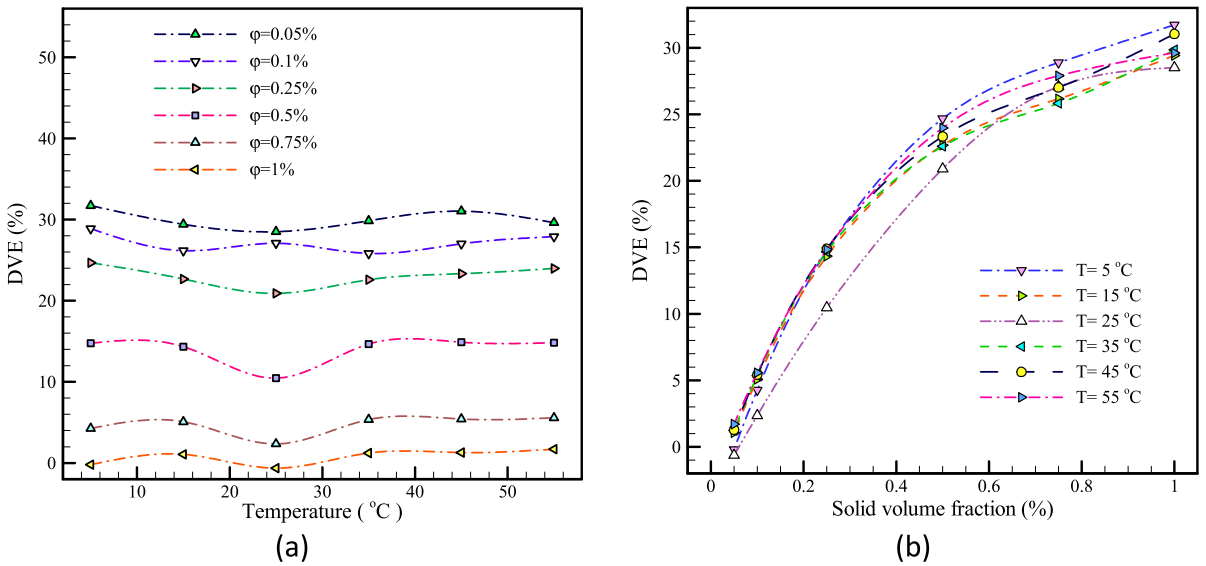

Fig. 9. Dynamic viscosity enhancement versus a) temperature and b) solid volume fraction.

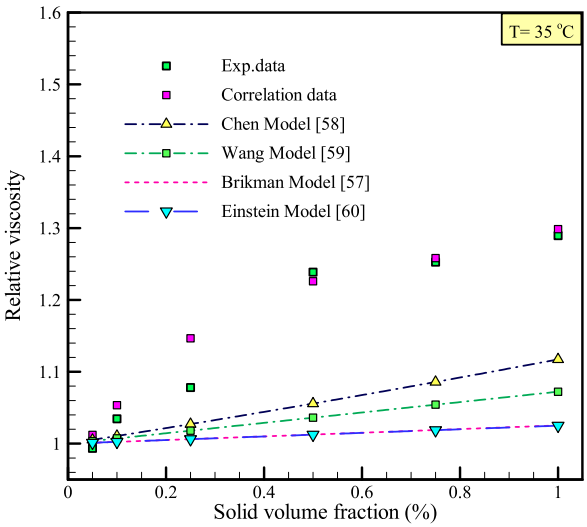

Fig. 10. Comparison between theoretical models & experimental data.

Table 10
Constant of variable for relative viscosity correlation of MWCNTs-SiO2(20–80)/10W40.

T	a_0	a_1	a_2	a_3
5	1.07845	0.9042	1.5319-	0.90614
15	1.08095	0.89177	1.57606-	0.93644
25	1.05788	1.34815	2.67134-	1.59605
35	1.09853	0.6678	1.07499-	0.64122
45	1.011047	0.55568	0.76709-	0.4435
55	1.09656	0.48617	0.55539-	0.33584
R-Squared	**>0.9800**			
Adj. R-Squared	**>0.9800**			

precision to predict the experimental data.

Fig. 11b has been drawn to show the precision of agreement between the predicted data and the experimental data. As the data get closer to the Equality line, it shows the high precision of the correlation for prediction. In this figure, a limited number of data are

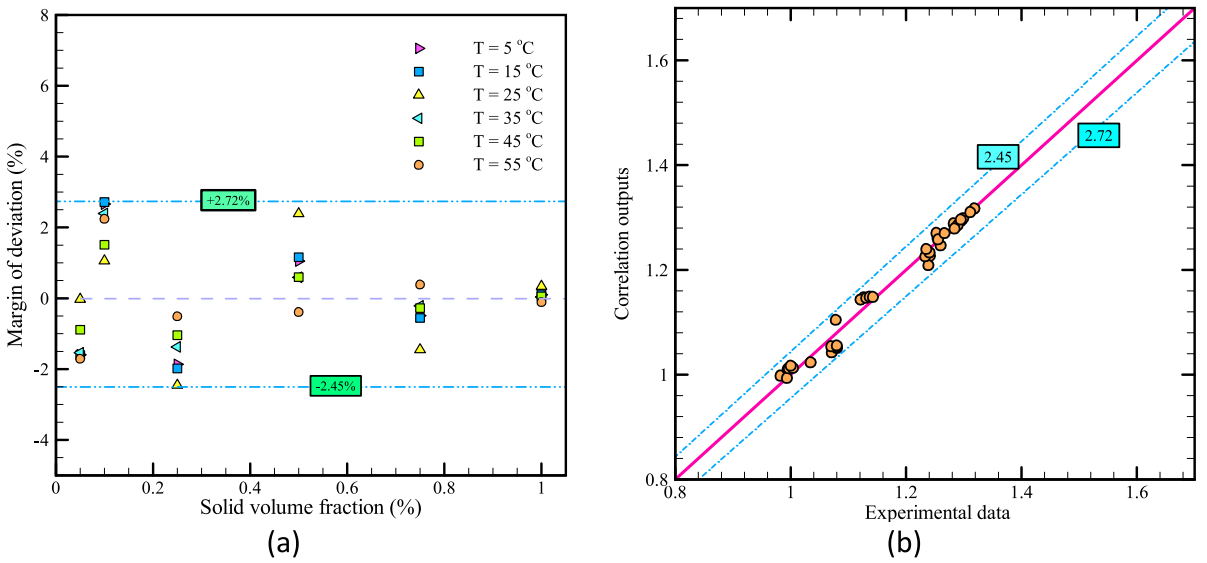

Fig. 11. a) Margin of deviation and b) Comparison between experimental data and correlation outputs.

located in a short distance from the bisector.

3.4. Sensitivity analyze

The dynamic viscosity values of different samples of the nano-lubricant in the study show a unique sensitivity to volume fraction variations. By using equation (8) [65], the sensitivity of MWCNT-SiO_2 (20%–80%)/10W40 hybrid nano-lubricant has been examined for 10% increase in nanoparticles.

$$\%Sensitivity = \left(\frac{\mu_{rel.}|_{After-Change}}{\mu_{rel.}|_{Base-Condition}} - 1 \right) \times 100 \tag{8}$$

In Fig. 12, the sensitivity of nano-lubricant viscosity has been drawn after increasing the volume fraction of 10%. As shown in the figure, the sensitivity of viscosity to volume fraction is much higher than temperature and it shows a variation of 0.3 unit of viscosity with increasing volume fraction. Nano-lubricants sensitivity analysis is effective of their design and utilization. When temperature variations are important, the nano-lubricants sensitivity with increasing volume fraction must be considered by designers.

4. Conclusion

In this study, the rheological behavior of hybrid nano-lubricant MWCNT-SiO_2 (20%–80%) 10W40 has been studied experimentally. Oxide nanoparticle has an average diameter of 20–30 nm and internal diameter of the carbon nanotube is 3–5 nm and its external diameter is 5–15 nm. For the homogeneous production and proper suspension of nano-lubricant, the usual two-step method and an ultrasonic device of 1200 W were used. The viscosity of samples in volume fractions of 0.05%, 0.1%, 0.25%, 0.5%, 0.75% and 1% and in temperatures of 5–55$^{\circ}C$ was analyzed. The study showed the following:

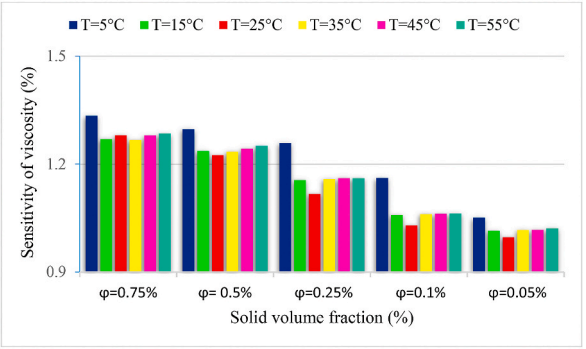

Fig. 12. Sensitivity of nano-lubricant versus solid volume fraction at various temperatures.

1. The rheological behavior of nano-lubricant follows Herschel-Bulkley model and it has non-Newtonian behavior of Bingham (pseudo-plastic) type in all temperatures except $55^{\circ}C$. Sometimes the behavior of nano-lubricant changes to dilatant.
2. Maximum percentage of deviation of nano-lubricant behavior from the ideal state of Bingham has been 15% toward pseudo-plastic and 10% toward dilatant.
3. In $55^{\circ}C$, increasing the volume fraction results in great changes in yield stress over to 100Pa. Also, at this temperature, "K" index value is close to zero in Herschel-Bulkley model and the behavior of nano-lubricant is just a function of yield stress.
4. The viscosity of nano-lubricant in the highest volume fraction (1%) and lowest temperature ($5^{\circ}C$) is over 1.3 times as big as that of pure oil and in the lowest volume fraction (0.05%) and highest temperature ($55^{\circ}C$) it is equal that.
5. Due to the small amount of viscosity sensitivity to volume fraction, adding nanoparticles to the lubricant in high temperatures does not show great changes in viscosity.
6. The maximum increase in dynamic viscosity of nano oil compared to pure oil (DVE) is about 32%. Increase in volume fraction leads to an increase in DVE.
7. Since relative viscosity data were not predicted by the present theoretical models, a new correlation with a very high precision was proposed. In this correlation, precision measurement index of R-squared is > 0.9700 and Adj. R-squared equals >0.9700. The maximum MOD in $55^{\circ}C$ and volume fraction of 0.1% is 2.72%.
8. Sensitivity analysis was conducted for engineering and systems designing applications, which shows an increase of 0.3 for increase in volume fraction.

Author contribution statement

Mousa Rejvani: Conceived and designed the experiments; Performed the experiments; Analyzed and interpreted the data; Contributed reagents, materials, analysis tools or data; Wrote the paper.

Alireza Heidari: Analyzed and interpreted the data; Contributed reagents, materials, analysis tools or data; Wrote the paper.

Seyfolah Seadodin: Conceived and designed the experiments; Analyzed and interpreted the data; Wrote the paper.

Funding statement

This research did not receive any specific grant from funding agencies in the public, commercial, or not-for-profit sectors.

Data availability statement

Data included in article/supp. material/referenced in article.

Declaration of interest's statement

The authors declare no conflict of interest.

Acknowledgements

The authors would like to acknowledge the Andishe Sazan-e-Sana't Ayande for their support and contribution to this study. We are grateful to the peer reviewers and editors for their valuable helpful suggestions, whose keen eyes made many constructive comments.

Nomenclature

K	Structure-dependent parameters
t	Structure-dependent parameters
T	Temperature (°C)
w	Weight (gr)

Greeks symbols

$\dot{\gamma}$	Shear rate (s^{-1})
μ	Dynamic viscosity (poise)
ρ	Density (kg/m^3)
T	Shear stress ($dyne/cm^2$)
φ	Nanoparticle volume fraction

Subscripts

b_f	Base fluid
n_f	Nanofluid

HB Herschel-Bulkley
OW Ostwald de Waele
Y Yield-stress

Appendix E. Supplementary data

Supplementary data related to this article can be found at https://doi.org/10.1016/j.heliyon.2023.e12942.

Appendix (Supporting information)

Table A
The R-squared value of Herschel-Bulkley equation fitted on shear stress-shear rate diagram.

R-squared	Solid volume fraction (%)						
T (°C)	1	0.75	0.5	0.25	0.1	0.05	0
5	1	1	1	1	1	1	1
15	1	1	1	1	1	1	1
25	1	1	0.9999	1	1	1	0.9999
35	1	1	1	0.9998	1	0.9987	0.9999
45	0.99994	0.9998	0.9997	0.9997	0.9992	0.9959	0.9995
55	0.9963	0.9964	0.9943	0.9763	0.9793	0.874	0.9994

Table B
The R-squared value of Ostwald de Waele equation fitted on shear stress-shear rate diagram.

R-squared	Solid volume fraction (%)						
T (°C)	1	0.75	0.5	0.25	0.1	0.05	0
5	1	1	1	1	1	1	1
15	1	1	1	1	1	1	1
25	1	1	0.9999	1	1	1	0.9999
35	1	1	1	0.9998	1	0.9987	0.9999
45	0.9994	0.9998	0.9997	0.9997	0.9992	0.9956	0.9995
55	0.996	0.9963	0.9939	0.9756	0.9793	0.874	0.9988

Table C
Difference R-squared value of Ostwald de Waele and Herschel-Bulkely equation

R-square (HB)- R-squared (OW)	Solid volume fraction (%)						
T (°C)	1	0.75	0.5	0.25	0.1	0.05	0
5	0	0	0	0	0	0	0
15	0	0	0	0	0	0	0
25	0	0	0	0	0	0	0
35	0	0	0	0	0	0	0
45	0	0	0	0	0	0.0003	0
55	0	0.0001	0.0004	0.0007	0	0	0.0006

References

[1] S.U.S. Choi, Enhancing thermal conductivity of fluids with nanoparticles, Proc. 1995 ASME Int. Mech. Eng. Congr. Expo. 66 (1995) 99–105.
[2] D. Zheng, J. Wang, Z. Chen, J. Baleta, B. Sunden, Performance analysis of a plate heat exchanger using various nanofluids, Int. J. Heat Mass Tran. 158 (2020), https://doi.org/10.1016/J.IJHEATMASSTRANSFER.2020.119993.
[3] H. Li, W. Sun, M. Zhu, P. Xue, Experimental study on the influence on vibration characteristics of thin cylindrical shell with hard coating under cantilever boundary condition, Shock Vib. 2017 (2017), https://doi.org/10.1155/2017/1751870.
[4] Z.R. Peng, Q.Y. Zheng, J. Chen, S.C. Yu, X.R. Zhang, Numerical investigation on heat transfer and pressure drop characteristics of coupling transcritical flow and two-phase flow in a printed circuit heat exchanger, Int. J. Heat Mass Tran. 153 (2020), https://doi.org/10.1016/J.IJHEATMASSTRANSFER.2020.119557.
[5] X. Zhao, X. Han, Y. Yao, J. Huang, Stability investigation of propylene glycol-based Ag@SiO2 nanofluids and their performance in spectral splitting photovoltaic/thermal systems, Energy 238 (2022), https://doi.org/10.1016/J.ENERGY.2021.122040.
[6] M. Chereches, A. Vardaru, G. Huminic, E.I. Chereches, A.A. Minea, A. Huminic, Thermal conductivity of stabilized PEG 400 based nanofluids: an experimental approach, Int. Commun. Heat Mass Tran. 130 (2022), 105798, https://doi.org/10.1016/J.ICHEATMASSTRANSFER.2021.105798.
[7] Y. Meng, J. Sun, J. He, F. Yang, P. Wu, Interfacial interaction induced synergistic lubricating performance of MoS2 and SiO2 composite nanofluid, Colloids Surfaces A Physicochem. Eng. Asp. 626 (2021), https://doi.org/10.1016/J.COLSURFA.2021.126999.
[8] L. Chen, H. Xie, Silicon oil based multiwalled carbon nanotubes nanofluid with optimized thermal conductivity enhancement, Colloids Surfaces A Physicochem. Eng. Asp. 352 (2009) 136–140, https://doi.org/10.1016/j.colsurfa.2009.10.015.
[9] S.U. Ilyas, R. Pendyala, N. Marneni, Stability and agglomeration of alumina nanoparticles in ethanol-water mixtures, Procedia Eng. 148 (2016) 290–297, https://doi.org/10.1016/j.proeng.2016.06.616.

[10] S. Fotowat, S. Askar, M. Ismail, A. Fartaj, A study on corrosion effects of a water based nanofluid for enhanced thermal energy applications, Sustain. Energy Technol. Assessments (2017) 1–6, https://doi.org/10.1016/j.seta.2017.02.001.

[11] G.M. Moatimid, M.A. Hassan, Convection instability of non-Newtonian Walter's nanofluid along a vertical layer, J. Egypt. Math. Soc. (2016) 1–10, https://doi.org/10.1016/j.joems.2016.09.001.

[12] A. Pramanik, H. Singh, R. Chandra, V.K. Vijay, S. Suresh, Amorphous carbon based nanofluids for direct radiative absorption in solar thermal concentrators – experimental and computational study, Renew. Energy 183 (2022) 651–661, https://doi.org/10.1016/J.RENENE.2021.11.047.

[13] T. Venkatesh, S. Manikandan, C. Selvam, S. Harish, Performance enhancement of hybrid solar PV/T system with graphene based nanofluids, Int. Commun. Heat Mass. Tran. 130 (2022), 105794, https://doi.org/10.1016/J.ICHEATMASSTRANSFER.2021.105794.

[14] C. Wang, J. Sun, C. Ge, H. Tang, P. Wu, Synthesis, characterization and lubrication performance of reduced graphene oxide-Al2O3 nanofluid for strips cold rolling, Coll. Surf. A Physicochem. Eng. Asp. 637 (2022), https://doi.org/10.1016/J.COLSURFA.2021.128204.

[15] S. Aberoumand, A. Jafarimoghaddam, Experimental study on synthesis, stability, thermal conductivity and viscosity of Cu–engine oil nanofluid, J. Taiwan Inst. Chem. Eng. 71 (2017) 315–322, https://doi.org/10.1016/j.jtice.2016.12.035.

[16] G. Zyla, J. Fal, Experimental studies on viscosity, thermal and electrical conductivity of aluminum nitride-ethylene glycol (AlN-EG) nanofluids, Thermochim. Acta 637 (2016) 11–16, https://doi.org/10.1016/j.tca.2016.05.006.

[17] M. Fakoor Pakdaman, M.A. Akhavan-Behabadi, P. Razi, An experimental investigation on thermo-physical properties and overall performance of MWCNT/heat transfer oil nanofluid flow inside vertical helically coiled tubes, Exp. Therm. Fluid Sci. 40 (2012) 103–111, https://doi.org/10.1016/j.expthermflusci.2012.02.005.

[18] M. Hemmat Esfe, A. Alirezaie, M. Rejvani, An applicable study on the thermal conductivity of SWCNT-MgO hybrid nanofluid and price-performance analysis for energy management, Appl. Therm. Eng. 111 (2017) 1202–1210, https://doi.org/10.1016/j.applthermaleng.2016.09.091.

[19] Y. Chen, P. Luo, Q. Tao, X. Liu, D. He, Natural convective heat transfer investigation of nanofluids affected by electrical field with periodically changed direction, Int. Commun. Heat Mass Tran. 128 (2021), https://doi.org/10.1016/J.ICHEATMASSTRANSFER.2021.105613.

[20] M. Rejvani, A. Alipour, S.M. Vahedi, A.J. Chamkha, S. Wongwises, Optimal characteristics and heat transfer efficiency of SiO_2/water nanofluid for application of energy devices: a comprehensive study, Int. J. Energy Res. 43 (2019), https://doi.org/10.1002/er.4854.

[21] K. Goudarzi, F. Nejati, E. Shojaeizadeh, S.K. Asadi Yousef-abad, Experimental study on the effect of pH variation of nanofluids on the thermal efficiency of a solar collector with helical tube, Exp. Therm. Fluid Sci. 60 (2015) 20–27, https://doi.org/10.1016/j.expthermflusci.2014.07.015.

[22] Y.H. Diao, C.Z. Li, J. Zhang, Y.H. Zhao, Y.M. Kang, Experimental investigation of MWCNT–water nanofluids flow and convective heat transfer characteristics in multiport minichannels with smooth/micro-fin surface, Powder Technol. 305 (2017) 206–216, https://doi.org/10.1016/j.powtec.2016.10.011.

[23] F. Gao, Y. Chen, J. Cai, C. Ma, Experimental study of free-surface jet impingement heat transfer with molten salt, Int. J. Heat Mass Tran. 149 (2020), https://doi.org/10.1016/J.IJHEATMASSTRANSFER.2019.119160.

[24] S.C. Godi, A. Pattamatta, C. Balaji, Heat transfer from a single and row of three dimensional wall jets - a combined experimental and numerical study, Int. J. Heat Mass Tran. 159 (2020), https://doi.org/10.1016/J.IJHEATMASSTRANSFER.2020.119801.

[25] M.H. Esfe, S. Alidust, E.M. Ardeshiri, D. Toghraie, Comparative rheological study of hybrid nanofluids with different base fluids and the same composition ratio to select the best performance of nano-lubricants using response surface modeling, Coll. Surf. A Physicochem. Eng. Asp. (2022), 128543, https://doi.org/10.1016/J.COLSURFA.2022.128543.

[26] M.Z. Saidi, C. El Moujahid, A. Pasc, N. Canilho, C. Delgado-Sanchez, A. Celzard, V. Fierro, R. Kouitat-Njiwa, T. Chafik, Enhanced tribological properties of wind turbine engine oil formulated with flower-shaped MoS2 nano-additives, Coll. Surf. A Physicochem. Eng. Asp. 620 (2021), https://doi.org/10.1016/J.COLSURFA.2021.126509.

[27] M. Hemmat Esfe, S. Alidoust, S. Esfandeh, D. Toghraie, E. Mohammadnejad Ardeshiri, Laboratory and statistical evaluations of rheological behaviour of MWCNT-Al2O3 (20:80)/Oil SAE50 as possible modified nano-lubricants, Coll. Surf. A Physicochem. Eng. Asp. 641 (2022), 128503, https://doi.org/10.1016/J.COLSURFA.2022.128503.

[28] B. Buonomo, O. Manca, L. Marinelli, S. Nardini, Effect of temperature and sonication time on nanofluid thermal conductivity measurements by nano-flash method, Appl. Therm. Eng. 91 (2015) 181–190, https://doi.org/10.1016/j.applthermaleng.2015.07.077.

[29] H.W. Chiam, W.H. Azmi, N.A. Usri, R. Mamat, N.M. Adam, Thermal conductivity and viscosity of Al2O3 nanofluids for different based ratio of water and ethylene glycol mixture, Exp. Therm. Fluid Sci. 81 (2017) 420–429, https://doi.org/10.1016/j.expthermflusci.2016.09.013.

[30] A. Joseph, S. Thomas, Energy, exergy and corrosion analysis of direct absorption solar collector employed with ultra-high stable carbon quantum dot nanofluid, Renew. Energy 181 (2022) 725–737, https://doi.org/10.1016/J.RENENE.2021.09.079.

[31] H. Chen, X. Chen, Y. Wu, Y. Lu, X. Wang, C. Ma, Experimental study on forced convection heat transfer of KNO3–Ca(NO3)2 + SiO2 molten salt nanofluid in circular tube, Sol. Energy 206 (2020) 900–906, https://doi.org/10.1016/j.solener.2020.06.061.

[32] B. Wang, X. Wang, W. Lou, J. Hao, Thermal conductivity and rheological properties of graphite/oil nanofluids, Coll. Surf. A Physicochem. Eng. Asp. 414 (2012) 125–131, https://doi.org/10.1016/j.colsurfa.2012.08.008.

[33] H. Abou-Ziyan, M. Mahmoud, R. Al-Ajmi, M. Shedid, Effects of synergetic and antagonistic additive elements on the thermal performance of engine oils at various bulk temperatures, Appl. Therm. Eng. 89 (2015) 618–627.

[34] H. Li, L. Wang, Y. He, Y. Hu, J. Zhu, B. Jiang, Experimental investigation of thermal conductivity and viscosity of ethylene glycol based ZnO nanofluids, Appl. Therm. Eng. 88 (2015) 363–368, https://doi.org/10.1016/j.applthermaleng.2014.10.071.

[35] L.S. Sundar, K.V. Sharma, M.T. Naik, M.K. Singh, Empirical and theoretical correlations on viscosity of nanofluids: a review, Renew. Sustain. Energy Rev. 25 (2013) 670–686, https://doi.org/10.1016/j.rser.2013.04.003.

[36] M. Hemmat Esfe, R. Karimpour, A.A. Abbasian Arani, J. Shahram, Experimental investigation on non-Newtonian behavior of Al 2 O 3 -MWCNT/5W50 hybrid nano-lubricant affected by alterations of temperature, concentration and shear rate for engine applications, Int. Commun. Heat Mass Tran. 82 (2017) 97–102, https://doi.org/10.1016/j.icheatmasstransfer.2017.02.006.

[37] M. Hemmat Esfe, H. Rostamian, Non-Newtonian power-law behavior of TiO 2/SAE 50 nano-lubricant: an experimental report and new correlation, J. Mol. Liq. 232 (2017) 219–225, https://doi.org/10.1016/j.molliq.2017.02.014.

[38] M. Hemmat Esfe, H. Rostamian, M. Reza Sarlak, M. Rejvani, A. Alirezaie, Rheological behavior characteristics of TiO2-MWCNT/10w40 hybrid nano-oil affected by temperature, concentration and shear rate: an experimental study and a neural network simulating, Phys. E Low-Dimensional Syst. Nanostructures (2017), https://doi.org/10.1016/j.physe.2017.07.012.

[39] M. Abdollahi-Moghaddam, M. Rejvani, P. Alamdari, Determining optimal formulations and operating conditions for Al2O3/water nanofluid flowing through a microchannel heat sink for cooling system purposes using statistical and optimization tools, Therm. Sci. Eng. Prog. 8 (2018) 517–524, https://doi.org/10.1016/j.tsep.2018.10.009.

[40] M.H. Esfe, S. Alidust, E.M. Ardeshiri, D. Toghraie, Comparative rheological study of hybrid nanofluids with different base fluids and the same composition ratio to select the best performance of nano-lubricants using response surface modeling, Coll. Surf. A Physicochem. Eng. Asp. (2022), 128543, https://doi.org/10.1016/J.COLSURFA.2022.128543.

[41] M. Hemmat Esfe, S. Saedodin, O. Mahian, S. Wongwises, Thermophysical properties, heat transfer and pressure drop of COOH-functionalized multi walled carbon nanotubes/water nanofluids, Int. Commun. Heat Mass Tran. 58 (2014) 176–183, https://doi.org/10.1016/j.icheatmasstransfer.2014.08.037.

[42] S. Areekara, F. Mabood, A.S. Sabu, A. Mathew, I.A. Badruddin, Dynamics of water conveying single-wall carbon nanotubes and magnetite nanoparticles subject to induced magnetic field: a bioconvective model for theranostic applications, Int. Commun. Heat Mass Tran. 126 (2021), https://doi.org/10.1016/J.ICHEATMASSTRANSFER.2021.105484.

[43] A. Hussain, A. Hassan, Q. Al Mdallal, H. Ahmad, A. Rehman, M. Altanji, M. Arshad, Heat transport investigation of magneto-hydrodynamics (SWCNT-MWCNT) hybrid nanofluid under the thermal radiation regime, Case Stud. Therm. Eng. 27 (2021), https://doi.org/10.1016/J.CSITE.2021.101244.

[44] R.U. Haq, S.S. Shah, E.A. Algehyne, I. Tlili, Heat transfer analysis of water based SWCNTs through parallel fins enclosed by square cavity, Int. Commun. Heat Mass Tran. 119 (2020), https://doi.org/10.1016/J.ICHEATMASSTRANSFER.2020.104797.

[45] M. Farbod, A. Ahangarpour, Improved thermal conductivity of Ag decorated carbon nanotubes water based nanofluids, Phys. Lett. 380 (2016) 4044–4048, https://doi.org/10.1016/j.physleta.2016.10.014.
[46] M.I. Asjad, M. Aleem, A. Ahmadian, S. Salahshour, M. Ferrara, New trends of fractional modeling and heat and mass transfer investigation of (SWCNTs and MWCNTs)-CMC based nanofluids flow over inclined plate with generalized boundary conditions, Chin. J. Phys. 66 (2020) 497–516, https://doi.org/10.1016/J.CJPH.2020.05.026.
[47] R. Yang, Y. Zheng, P. Li, H. Bai, Y. Wang, L. Chen, Effects of acidification time of MWCNTs on carbon dioxide capture of liquid-like MWCNTs organic hybrid materials, RSC Adv. 6 (2016) 85970–85977, https://doi.org/10.1039/C6RA16909K.
[48] A. Samadzadeh, S. Zeinali Heris, Effect of stabilization method on the natural convection in an inclined cavity filled with MWCNTs/water nanofluids, Int. Commun. Heat Mass Tran. 129 (2021), 105645, https://doi.org/10.1016/J.ICHEATMASSTRANSFER.2021.105645.
[49] M.R. Esfahani, E.M. Languri, Exergy analysis of a shell-and-tube heat exchanger using graphene oxide nanofluids, Exp. Therm. Fluid Sci. 83 (2017) 100–106, https://doi.org/10.1016/j.expthermflusci.2016.12.004.
[50] J. Li, X. Zhang, B. Xu, M. Yuan, Nanofluid research and applications: a review, Int. Commun. Heat Mass Tran. 127 (2021), https://doi.org/10.1016/J.ICHEATMASSTRANSFER.2021.105543.
[51] G. Wang, Y. Yang, S. Wang, Thermophysical properties analysis of graphene-added phase change materials and evaluation of enhanced heat transfer effect in underwater thermal vehicles, J. Mol. Liq. (2021), 118048, https://doi.org/10.1016/J.MOLLIQ.2021.118048.
[52] A. Khose, S. Kolhe, V.N. Deshmukh, Investigations on the effect of graphene coating on thermophysical properties of aluminium and mild steel for cross flow heat exchanger, Mater. Today Proc. (2021), https://doi.org/10.1016/J.MATPR.2021.10.166.
[53] J. Zhou, X. Luo, B. He, C. Li, L. Liang, Z. Yin, Z.Q. Tian, Comprehensive evaluation of graphene/R141b nanofluids enhanced heat transfer performance of minichannel heat sinks, Powder Technol. (2021), https://doi.org/10.1016/J.POWTEC.2021.11.041.
[54] L. Yang, K. Du, S. Bao, Y. Wu, Investigations of selection of nanofluid applied to the ammonia absorption refrigeration system, Int. J. Refrig. 35 (2012) 2248–2260, https://doi.org/10.1016/j.ijrefrig.2012.08.003.
[55] M. Hemmat Esfe, M.R. Hassani Ahangar, M. Rejvani, D. Toghraie, M.H. Hajmohammad, Designing an artificial neural network to predict dynamic viscosity of aqueous nanofluid of TiO2 using experimental data, Int. Commun. Heat Mass Tran. 75 (2016) 192–196, https://doi.org/10.1016/j.icheatmasstransfer.2016.04.002.
[56] M.H. Esfe, S. Wongwises, M. Rejvani, Prediction of thermal conductivity of carbon nanotube-EG nanofluid using experimental data by ANN, Curr. Nanosci. 13 (2017), https://doi.org/10.2174/1573413713666161213114458.
[57] M. Rejvani, S. Saedodin, S.M. Vahedi, S. Wongwises, A.J. Chamkha, Experimental investigation of hybrid nano-lubricant for rheological and thermal engineering applications, J. Therm. Anal. Calorim. 1382 (2019) 1823–1839, https://doi.org/10.1007/S10973-019-08225-5.
[58] W.H. Herschel, R. Bulkley, Konsistenzmessungen von Gummi-Benzoll??sungen, Kolloid Z. 39 (1926) 291–300, https://doi.org/10.1007/BF01432034.
[59] W.J. Tseng, K. Lin, Rheology and colloidal structure of aqueous TiO 2 nanoparticle suspensions, Mater. Sci. Eng. 355 (2003) 186–192, https://doi.org/10.1016/S0921-5093(03)00063-7.
[60] E. o llah Ettefaghi, H. Ahmadi, A. Rashidi, A. Nouralishahi, S.S. Mohtasebi, Preparation and thermal properties of oil-based nanofluid from multi-walled carbon nanotubes and engine oil as nano-lubricant, Int. Commun. Heat Mass Tran. 46 (2013) 142–147, https://doi.org/10.1016/j.icheatmasstransfer.2013.05.003.
[61] H.C. Brinkman, The viscosity of concentrated suspensions and solutions, J. Chem. Phys. 20 (1952) 571.
[62] H. Chen, Y. Ding, C. Tan, Rheological behaviour of nanofluids, New J. Phys. 9 (2007) 367, https://doi.org/10.1088/1367-2630/9/10/367.
[63] X. Wang, X. Xu, S.U.S. Choi, Thermal conductivity of nanoparticle - fluid mixture, J. Thermophys. Heat Tran. 13 (1999) 474–480, https://doi.org/10.2514/2.6486.
[64] A. Einstein, Eine neue bestimmung der moleküldimensionen, Ann. Phys. 324 (1906) 289–306, https://doi.org/10.1002/andp.19063240204.
[65] O. Mahian, A. Kianifar, S. Wongwises, Dispersion of ZnO nanoparticles in a mixture of ethylene glycol–water, exploration of temperature-dependent density, and sensitivity analysis, J. Cluster Sci. 24 (2013) 1103–1114, https://doi.org/10.1007/s10876-013-0601-4.
[66] M. Tajik Jamal-Abad, M. Dehghan, S. Saedodin, M.S. Valipour, A. Zamzamian, An experimental investigation of rheological characteristics of non-Newtonian nanofluids, J. Heat Mass Transf. Res. 1 (2014) 17–23.
[67] B. Wang, X. Wang, W. Lou, J. Hao, Rheological and tribological properties of ionic liquid-based nanofluids containing functionalized multi-walled carbon nanotubes, J. Phys. Chem. C 114 (2010) 8749–8754.
[68] M. Abareshi, S.H. Sajjadi, S.M. Zebarjad, E.K. Goharshadi, Fabrication, characterization, and measurement of viscosity of α-Fe 2 O 3-glycerol nanofluids, J. Mol. Liq. 163 (2011) 27–32.
[69] H. Chen, Y. Ding, A. Lapkin, X. Fan, Rheological behaviour of ethylene glycol-titanate nanotube nanofluids, J. Nanoparticle Res. 11 (2009) 1513–1520, https://doi.org/10.1007/s11051-009-9599-9.
[70] M. Afrand, D. Toghraie, B. Ruhani, Effects of temperature and nanoparticles concentration on rheological behavior of Fe 3 O 4–Ag/EG hybrid nanofluid: an experimental study, Exp. Therm. Fluid Sci. 77 (2016) 38–44, https://doi.org/10.1016/j.expthermflusci.2016.04.007.
[71] M. Kole, T.K. Dey, Thermal conductivity and viscosity of Al2O3 nanofluid based on car engine coolant, J. Phys. D Appl. Phys. 43 (2010), 315501.
[72] H. Eshgarf, M. Afrand, An experimental study on rheological behavior of non-Newtonian hybrid nano-coolant for application in cooling and heating systems, Exp. Therm. Fluid Sci. 76 (2016) 221–227, https://doi.org/10.1016/j.expthermflusci.2016.03.015.
[73] C. Sun, B. Bai, W.-Q. Lu, J. Liu, Shear-rate dependent effective thermal conductivity of H2O+ SiO2 nanofluids, Phys. Fluids 25 (2013), 52002.
[74] J. Glory, M. Bonetti, M. Helezen, M. Mayne-Lhermite, C. Reynaud, Thermal and electrical conductivities of water-based nanofluids prepared with long multiwalled carbon nanotubes, J. Appl. Phys. 103 (2008), 94309.
[75] M. Hemmat Esfe, A. Naderi, M. Akbari, M. Afrand, A. Karimipour, Evaluation of thermal conductivity of COOH-functionalized MWCNTs/water via temperature and solid volume fraction by using experimental data and ANN methods, J. Therm. Anal. Calorim. 121 (2015) 1273–1278.
[76] C. Pang, J.-Y. Jung, J.W. Lee, Y.T. Kang, Thermal conductivity measurement of methanol-based nanofluids with Al 2 O 3 and SiO 2 nanoparticles, Int. J. Heat Mass Tran. 55 (2012) 5597–5602.